Journal homepage: www.scienceletters.researchfloor.org

Journal of e-Science Letters

Review Article | ISSN 3041-5454

A Review on Synthesis of some Metal Oxide Nanoparticles by Sol-Gel Technique and its applications

Valarmathy Joshua*[1], L. Samuel Joshua[1], Sherlyn Joshua[2] and Vinolyn Joshua[2]

[1]*Medicinal Chemistry Research Laboratory, Department of Pharmaceutical Chemistry, Sri Venkateswaraa Faculty of Pharmacy, Ettayapuram -628902, Tamil Nadu, India*
[2]*UV Gullas College of Medicine, 6014 Mandaue City, Cebu, Philippines*

ABSTRACT

The sol-gel technique has emerged as a convenient and versatile method for the synthesis of metal oxide nanoparticles using various precursors such as metal alkoxides, metallo-organic salts, and inorganic salts in suitable solvents. Compared with conventional nanoparticle synthesis methods, the sol-gel process is economical, flexible, less complex, and can be carried out at relatively low temperatures. This technique offers excellent control over particle size, purity, homogeneity, and morphology. Sol-gel-derived materials have wide-ranging applications in medicine, biology, catalysis, electronics, cosmetics, antimicrobial therapy, drug delivery, and environmental sciences. This review summarizes the principles of the sol-gel process, sequential synthesis steps, preparation of selected metal oxide nanoparticles, and their important biomedical and industrial applications.

Keywords: *Metal oxide nanoparticles, Sol-gel technique, Nanotechnology, Biomedical applications, antimicrobial activity, Drug delivery.*

1. Introduction

The sol-gel process [1] is an important wet-chemical method used for the synthesis of nanoparticles and advanced materials. In this process, metal ions are dissolved either as alkoxides, metallo-organic compounds, or inorganic salts in suitable solvents such as alcohol or water. These precursors undergo hydrolysis, condensation, and polymerization reactions, resulting in the formation of highly condensed three-dimensional network structures known as gels. The term "sol-gel" originates from the transformation of a colloidal suspension (sol) into a semi-rigid network (gel). Sol-gel processing differs from precipitation methods because it stabilizes a finely dispersed colloidal phase in solution. Typically, the formation of metal oxides through the sol-gel route involves the formation of M–O–M or M–OH–M bridges, leading to metal-oxo or metal-hydroxo polymers.

Citation: Valarmathy Joshua, L. Samuel Joshua, Sherlyn Joshua and Vinolyn Joshua (2026). A Review on Synthesis of some Metal Oxide Nanoparticles by Sol-Gel Technique and its applications. *Journal of e-Science Letters.*
DOI: https://doi.org/10.51470/eSL.2026.7.1.105

Received: 17 November 2025
Revised: 23 December 2025
Accepted: 11 January 2026
Available: February 14 2026

Corresponding Authors: **Valarmathy Joshua**
Email: **valarmathyjoshua@gmail.com**

The major advantages of the sol-gel method include:
A. Low-temperature processing
B. High purity and homogeneity
C. Better control of particle size and morphology
D. Uniform composition
E. Cost-effectiveness
F. Easy fabrication of films, fibers, powders, and coatings

Because of these advantages, the sol-gel method is extensively applied in the preparation of metal oxide nanoparticles such as silver oxide, silica oxide, zinc oxide, iron oxide, alumina, copper oxide, and titanium oxide nanoparticles.

1. Sol-gel process

The sol-gel process[2] is a wet-chemical technique used for the fabrication of materials at relatively low temperatures. It begins either with a chemical solution or with colloidal particles (sol), which subsequently form an interconnected three-dimensional network known as a gel. In general, the sol-gel process involves three major stages: preparation of the sol, gelation of the sol, and removal of the solvent. The overall sol-gel process can be represented by the following sequence of transformations:

Precursor → Sol → Gel → Product

Precursors: Precursors are starting materials that contain the required metal ions in the desired stoichiometric ratio. Common precursors include:
A. Metal alkoxides
B. Metal chlorides
C. Metal nitrates

Sol: A sol is a colloidal suspension of particles in a liquid medium. The particle size generally ranges from 1 to 100 nm.

Gel: A gel is a semi-rigid three-dimensional network containing both solid and liquid phases. Gels may be:

- Colloidal gels
- Polymeric gels

2. Sequential Steps Involved in Sol-Gel Synthesis

Hydrolysis

Hydrolysis involves the reaction of inorganic or organometallic precursors with water or suitable solvents at ambient or slightly elevated temperatures. Acidic or basic catalysts are often added to accelerate the reaction.

Polymerization (Condensation)

In this step, adjacent molecules undergo condensation reactions in which water or alcohol is eliminated, leading to the formation of metal–oxide linkages. As the reaction progresses, polymeric networks grow to colloidal dimensions in the liquid (sol) state.

Gelation

Gelation results in the formation of a three-dimensional network throughout the liquid medium due to the interconnection of polymeric chains, converting the sol into a semi-rigid gel.

Ageing

Ageing refers to the continuous structural and property changes occurring in a gel that remains immersed in liquid after gel formation and before solvent removal. During ageing, smaller polymeric units gradually aggregate into the main network structure. Solvent molecules remain trapped within the pores of the gel, while prolonged ageing may lead to gel shrinkage.

Drying

Drying involves the removal of solvent at moderate temperatures (generally below 200 °C), leaving behind the solid residue. During this process, the gel shrinks because of the loss of pore fluid and maintenance of the liquid–vapour interface at the external surface of the gel.

Xerogel Formation

Conventional evaporative drying, such as oven heating, creates capillary pressure within the pores, which may collapse the porous network. The resulting material is called a xerogel, characterized by relatively low surface area and pore volume.

Aerogel Formation

In supercritical drying, capillary stress is minimized, preventing collapse of the porous structure. The resulting material, known as an aerogel, possesses high pore volume, large surface area, and low bulk density.

Cryogel Formation

Freeze drying of solvents at low temperature under reduced pressure produces cryogels. This method is similar to the lyophilization process widely used in the pharmaceutical industry.

Sonogel Formation

When the gel is subjected to ultrasonic vibrations at room temperature for solvent removal, the resulting material is termed a sonogel.

Drying Control Chemical Agents (DCCAs)

Drying control chemical agents significantly influence the texture, porosity, and morphology of the particles. Commonly used DCCAs include:

A. Formamide
B. Glycerol
C. Oxalic acid

Calcination

Calcination temperature plays an important role in controlling the pore size, crystallinity, density, and overall properties of the synthesized materials.

Figure 1: Sequential steps involved in the sol-gel process

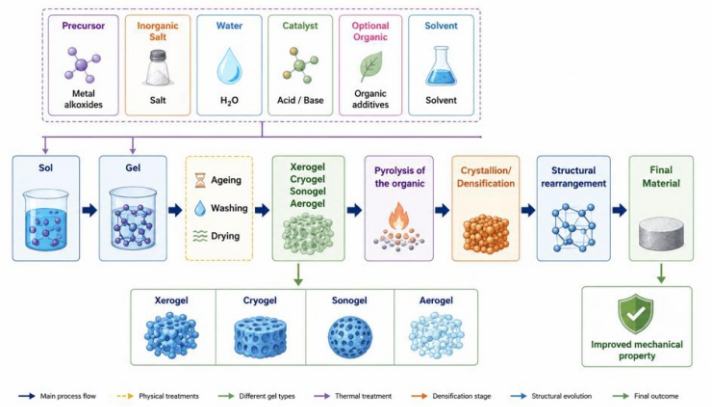

3. Synthesis of Some Metal Oxide Nanoparticles by Sol-Gel Technique

3.1 Synthesis of Silver Oxide Nanoparticles[3] by Sol-Gel Technique (Ag_2O)

Materials and Methods

Silver nitrate ($AgNO_3$) procured from Loba Chemicals was used as the precursor material. Analytical-grade ethanol, acetic acid (CH_3COOH), sodium hydroxide (NaOH), hydrazine hydrate ($N_2H_4 \cdot H_2O$), and ammonia solution were used without further purification. Deionized water (DIW) was used throughout the experiment. Initially, 100 mL aqueous solutions of $AgNO_3$ with concentrations of 6 mM, 7 mM, and 8 mM were prepared separately. A mixture containing 0.1 M acetic acid and 0.1 M sodium hydroxide in a 1:1 ratio was added to each solution. The pH of the resulting solution was gradually adjusted to 7 by the slow addition of ammonia solution under vigorous stirring. Subsequently, hydrazine hydrate solutions of concentrations 12 mM, 16 mM, and 20 mM were added separately to prepare three different samples. The solutions were stirred vigorously throughout the process. Upon addition of hydrazine hydrate, the solution turned black, indicating the reduction of silver ions and formation of silver oxide nanoparticles. The reaction mixture was continuously stirred for 3 hours at room temperature. After completion of the reaction, the solution became transparent with visible shining silver particles inside the flask. The synthesized nanoparticles were collected by filtration, washed several times with

$$2AgNO_3(aq) + CH_3COONa(aq) \rightarrow Ag_2O(s) + 2NaNO_3(aq) + CH_3COOH(l)$$

Table 1: Particle size of Silver oxide nanoparticles

Sample	MixerSolution ($AgNO_3$mixture+$N_2H_4.H_2O$)	Particle size(nm)
1.	6 mM +12 mM	6.22
2.	7 mM +16 mM	19.19
3.	8 mM +20 mM	22.50

$AgNO_3$ mixture (1:1): 100 ml of aqueous solution of $AgNO_3$ (6mM, 7mM, and 8mM) , 0.1 M of acetic acid with 0.1Msodium hydroxide and NH_3 solution was added at pH 7and stirred vigorously.

3.2 Synthesis of Silica Oxide Nanoparticles by Sol-Gel Technique (SiO_2) [4]

Materials and Methods

Tetraethyl orthosilicate [Si $(OC_2H_5)_4$] (TEOS) procured from Loba Chemicals was used as the precursor material. Analytical-grade ethanol (C_2H_5OH) and acetic acid (CH_3COOH) were used without further purification. Deionized water (DIW) was used throughout the study.

A 0.086 M solution of tetraethyl orthosilicate (18 mL) was mixed with 72 mL of deionized water and added to a 0.6 M acetic acid solution (36 mL) containing 6.4 mL of distilled water as the solvent system. The mixture was stirred thoroughly to obtain a homogeneous solution. The ageing time for the prepared sols was varied to 2, 4, and 6 hours. The resulting colloidal sol was then centrifuged and washed with 20 mL of ethanol, followed by repeated centrifugation to remove impurities. The obtained precipitate was dried at 60 °C for 24 hours. Subsequently, the dried material was calcined at temperatures of 600 °C and 700 °C for 1 hour and 30 minutes to obtain white silica nano powder.

$$Si(OC_2H_5)_4 + 4H_2O \rightarrow Si(OH)_4 + 4C_2H_5OH$$
$$Si(OH)_4 \rightarrow SiO_2 + 2H_2O$$

Figure 2: Process Flow of Silica Oxide Nanoparticle by Sol–Gel Technique

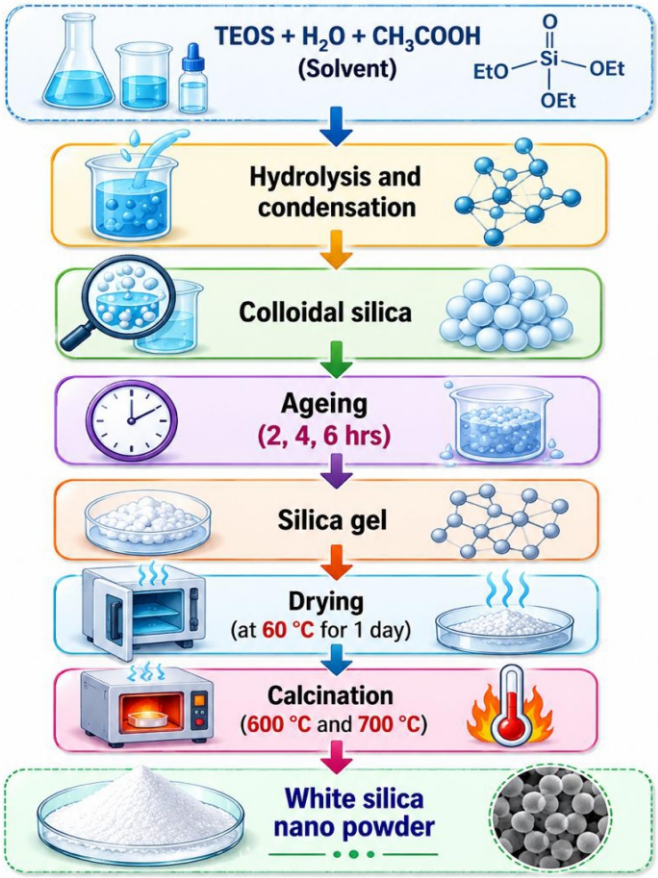

3.3 Synthesis of Zinc Oxide Nanoparticles[5] by Sol-Gel Technique (ZnO)

Materials and Methods

Zinc acetate dihydrate [Zn $(CH_3COO)_2{\cdot}2H_2O$] (≥99% purity) procured from HmbG Chemicals was used as the precursor material. Sodium hydroxide (NaOH, ≥98%, Sigma-Aldrich), ethanol (C_2H_5OH, HmbG Chemicals), and deionized water (DIW) were used throughout the study. To prepare the precursor solution, 2 g of zinc acetate dihydrate was dissolved in 15 mL of distilled water. Separately, 8 g of sodium hydroxide was dissolved in 10 mL of distilled water. Both solutions were stirred continuously for approximately 5 minutes to obtain homogeneous mixtures. The sodium hydroxide solution was then slowly added to the zinc acetate solution under constant stirring using a magnetic stirrer for about 5 minutes. Subsequently, 100 mL of ethanol was added dropwise to the reaction mixture using a burette. After completion of the reaction, a white precipitate was formed, indicating the formation of zinc oxide nanoparticles. The white precipitate was collected, washed thoroughly with deionized water and ethanol to remove impurities, and then dried to obtain ZnO nanoparticles.

$$Zn(CH_3COO)_2{\cdot}2H_2O + 2NaOH \rightarrow ZnO + 2CH_3COONa + 3H_2O$$

3.4 Synthesis of Iron Oxide Nanoparticles [6,7] by Sol-Gel Technique (Fe_3O_4 / Fe_2O_3)

Synthesis of Fe_3O_4 Nanoparticles

Materials and Methods

Iron (III) chloride hexahydrate ($FeCl_3{\cdot}6H_2O$), iron (II) chloride tetrahydrate ($FeCl_2{\cdot}4H_2O$), and ethylene glycol [$C_2H_6O_2$ or $(CH_2OH)_2$] of analytical grade were procured from Sigma-Aldrich Chemical Company. All reagents were used without further purification. Initially, 2.35 g of iron (III) chloride and 8.35 g of iron (II) chloride were dissolved in 60 mL of ethylene glycol and stirred vigorously for 3 hours at 45 °C to form a homogeneous solution. The prepared sol was then heated and maintained at 80 °C until a dark-colored gel was formed. The obtained gel was aged for 72 hours and subsequently dried at 140 °C for 5 hours. The resulting xerogel was annealed at temperatures ranging from 200 °C to 400 °C under vacuum conditions to obtain magnetite (Fe_3O_4) nanoparticles of different particle sizes. Finally, the synthesized Fe_3O_4 nanoparticles were washed several times with acetone and ethanol to remove impurities and dried properly.

$$4FeCl_3{\cdot}6H_2O + 3O_2 \rightarrow 2Fe_2O_3 + 12HCl + 18H_2O$$
$$5FeCl_2{\cdot}4H_2O + 2.5O_2 \rightarrow Fe_3O_4 + Fe_2O_3 + 10HCl + 15H_2O$$

Thus, high-temperature hydrolysis of $FeCl_3{\cdot}6H_2O$ and $FeCl_2{\cdot}4H_2O$ in the presence of oxygen leads to the formation of ultrafine iron oxide powders, predominantly Fe_3O_4 nanoparticles.

Table 2: Particle Size of Fe_3O_4 Nanoparticles

Sample	Calcination temperature (^{0}C)	particle size (nm)
1.	200	2.02
2.	300	5.58
3.	400	8.35

Synthesis of Fe_2O_3 Nanoparticles

Materials and Methods

Iron nitrate [$Fe(NO_3)_3 \cdot 6H_2O$] (Aldrich, 98%) and monohydrated citric acid (Aldrich, 98%) were used as precursor and ligand materials, respectively. A 200 mL solution of 0.1 M iron nitrate was prepared and gelated using 800 mL monohydrated citric acid solution (0.05–0.2 M) in distilled water. The iron nitrate solution was added dropwise into the citric acid solution under vigorous stirring. The resulting mixture was heated to 70 °C while continuously stirring until gel formation occurred and the solvent evaporated completely. The dried gel was then annealed at temperatures ranging from 180 °C to 400 °C, producing approximately 1.6 g of Fe_2O_3 nanoparticles with particle sizes ranging from 22–56 nm.

$$Fe(NO_3)_3 \cdot 6H_2O \rightarrow Fe_2O_3 + 12HNO_3 + 18H_2O$$

Table 3: Particle Size of Fe_2O_3 Nanoparticles

Sample	Calcination temperature (0C)	particle size (nm)
1.	180	36
2.	210	33
3.	230	31
4.	250	24
5.	400	22

Note: *All samples were prepared using a 0.1 M citric acid concentration.*

3.5 Synthesis of Alumina Nanoparticles[8] by Sol-Gel Technique (Al_2O_3)

Materials and Methods

Acetylacetone (ACA), ethyl acetoacetate (EACA), and acetic acid (Ac) of analytical grade were procured from Merck Company (Germany). Ethanol of two different purities, 96% and 99.99%, was used throughout the investigation.

(a) Sol-Gel Method Using ACA Chelating Agent (ACA)

Initially, 24 g of $AlCl_3 \cdot 6H_2O$ was added to 100 mL of ethanol and stirred for 2.5 hours to obtain a primary gel. Subsequently, 10.5 mL of acetylacetone was added, and stirring was continued for another 3 hours to obtain a xerogel. The xerogel was dried in an oven at 120 °C for approximately 48 hours. The dried material was then sintered at 1000 °C for 3 hours to convert γ-Al_2O_3 into stable α-Al_2O_3. A porous, low-density white material was obtained, which was finally ground using a ball mill to produce alumina nanopowder.

(b) Sol-Gel Method Using ACA Chelating Agent with Reduced Stirring Speed (ACA-RSS)

In this method, 24 g of $AlCl_3 \cdot 6H_2O$ was dissolved in 100 mL of ethanol with stirring for 2.5 hours. Then, 10.5 mL acetylacetone was added, and stirring was continued for 4 hours. The stirring speed was reduced to half of that used in the previous process to study its effect on gel formation. Since no major changes occurred after 13 hours of stirring, the sol was allowed to stand undisturbed for 24 hours. Stirring was then resumed at 70 °C for 6 hours to obtain the xerogel. Drying at 120 °C required a longer duration compared with the previous method. Subsequent processing steps were similar, resulting in the formation of α-Al_2O_3 nanoparticles.

(c) Sol-Gel Method Using ACA with Increased Amount of Solvent (ACA-IAS)

This method followed the previous procedure, except that the amount of ethanol solvent was doubled. The increased solvent volume prolonged the time required for primary gel formation. The remaining preparation steps were identical, resulting in the formation of Al_2O_3 nanoparticles.

(d) Sol-Gel Method Using ACA with Increased Solvent and Addition of Water (ACA-IAS + Water)

In this method, the amount of ethanol was increased to 200 mL. After sol formation, 10 mL of distilled water was added under continuous stirring at 70 °C. The addition of water significantly reduced gel formation time compared with the previous methods. The subsequent drying and calcination steps were carried out similarly, producing Al_2O_3 nanoparticles.

(e) Sol-Gel Method Using EACA Chelating Agent (EACA)

In this process, 24 g of $AlCl_3 \cdot 6H_2O$ was dissolved in 100 mL of ethanol and stirred for 2.5 hours to form a primary gel. Then, 10 mL ethyl acetoacetate was added. The mixture was stirred for approximately 13 hours until a transparent and colorless gel formed. Stirring was then stopped, and the solution was left undisturbed for 24 hours, producing a white colloidal gel. Restirring was continued for 2 hours, followed by drying and calcination steps similar to previous methods to obtain alumina nanopowder.

(f) Sol-Gel Method Using EACA Chelating Agent and Acetic Acid (EACA + Ac)

This method was similar to the previous experiment, except that 10 mL of acetic acid was added along with ethyl acetoacetate to prepare the primary gel under acidic conditions. This experiment was conducted to investigate the influence of pH on gel formation. Subsequent procedures for nanoparticle preparation were similar to those described earlier, resulting in the formation of alumina nanoparticles. The synthesized alumina nanoparticles appeared as fine white nanopowders after calcination and milling.

$$2AlCl_3 + 3H_2O \rightarrow Al_2O_3 + 6HCl$$

Figure 3. Flowchart for the synthesis of aluminum oxide nanoparticles (Al_2O_3) using the sol–gel technique.

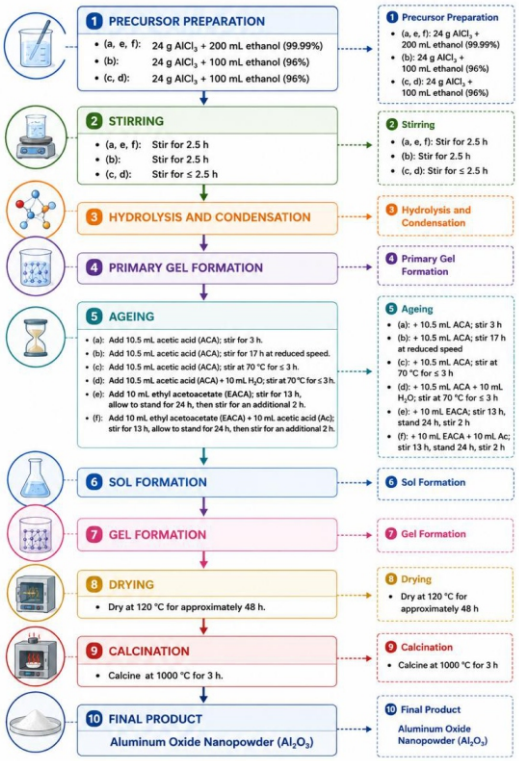

Table 5: The particle size of Aluminum oxide nanoparticles uses either acetylacetone or ethyl acetoacetate as chelating agents

Sample	Product	particle size (nm)
ACA	γ-Al_2O_3	37.37
ACA-RSS	α-Al_2O_3	38.63
ACA-IAS	γ-Al_2O_3	5.32
ACA-IAS +Water	γ-Al_2O_3	5.59
EACA	α-Al_2O_3	35.43
EACA+Ac	α-Al_2O_3	36.38

3.6. Synthesis of Copper Oxide Nanoparticles by Sol–Gel Technique (CuO) [9-10]

Materials and Methods

Copper chloride dihydrate ($CuCl_2 \cdot 6H_2O$) was procured from Loba Chemicals. Analytical grade ethanol (C_2H_5OH) and sodium hydroxide (NaOH) were used in the study. Deionized water (DIW) was used throughout the experiments. In the synthesis procedure, 0.9 g of copper (II) chloride was dissolved in 25 mL of ethanol, while 1.5 g of sodium hydroxide was dissolved in 80 mL of ethanol. The sodium hydroxide solution was added dropwise to the copper chloride solution under constant stirring at room temperature for 30 minutes. During the reaction, the colour of the solution changed from dark blue to black, indicating the formation of copper oxide nanoparticles. The resulting gel was filtered using filter paper and washed thoroughly with water. The sample was then dried at room temperature and annealed at 700 °C using a Carbolite CWF 1200 laboratory chamber furnace. Finally, the annealed copper oxide nanoparticles were ground into fine powder.

$$CuCl_2 \cdot 6H_2O + 2NaOH \rightarrow Cu(OH)_2 + 2NaCl + 6H_2O$$
$$Cu(OH)_2 \rightarrow CuO + H_2O$$

Alternative Sol–Gel Method for CuO Nanoparticles

All chemicals, including $CuSO_4 \cdot 7H_2O$, Tween 80, NaOH, and soybean oil. All reagents were of analytical grade and used without further purification. In this method, 0.80 g of $CuSO_4 \cdot 7H_2O$ dissolved in 3 mL of water and 6.5% Tween 80 were added to 80 mL of purified soybean oil under mechanical stirring at 2500 rpm until a nearly clear emulsion was obtained. This mixture was designated as Solution A. Separately, 0.45 g of NaOH was dissolved in 2.8 mL of water and added to Solution A under continuous mechanical stirring at 2100 rpm for 3.5 hours at room temperature. The reaction mixture was then filtered, and the precipitate was washed four times with distilled water (3 × 600 mL). The obtained material was calcined in an electric oven at 220 °C for 5 hours. This technique enabled the preparation of ultrafine CuO nanoparticles with particle sizes ranging from 50–60 nm.

$$CuSO_4 \cdot 7H_2O + 2NaOH \rightarrow Cu(OH)_2 + Na_2SO_4 + 7H_2O$$
$$Cu(OH)_2 \rightarrow CuO + H_2O$$

3.7. Synthesis of Titanium Oxide Nanoparticles by Sol–Gel Technique (TiO_2) [16-17]

Materials and Methods

Titanium tetrachloride ($TiCl_4$, 99.99%, BDH, England) and absolute ethanol (C_2H_5OH, 99.99%, GCC, U.K.) were used as precursor materials. In the synthesis procedure, 14 mL of titanium tetrachloride was added slowly in a dropwise manner into 140 mL of absolute ethanol under continuous stirring at room temperature. The reaction was carried out inside a chemical fume hood due to the evolution of chlorine (Cl_2) and hydrochloric acid (HCl) gases during the reaction. The resulting yellow solution was allowed to stand and cool to room temperature after cessation of gas evolution. The pH of the solution was maintained in the range of 1–2. The obtained suspension was dried in an oven at 80 °C for several hours until amorphous dried TiO_2 particles were formed. The dried powder samples were then calcined in a box furnace at temperatures ranging from 550–600 °C for 2 hours under ambient atmospheric conditions. After calcination, the powder transformed into TiO_2 nanoparticles in the anatase phase.

$$TiCl_4 + 4C_2H_5OH \rightarrow Ti(OC_2H_5)_4 + 4HCl$$
$$Ti(OC_2H_5)_4 + 2H_2O \rightarrow TiO_2 + 4C_2H_5OH$$

Alternative Sol–Gel Method Using Titanium Tetra Isopropoxide (TTIP)

Materials and Methods

Titanium tetra isopropoxide [$Ti(OCH(CH_3)_2)_4$] (TTIP, Sigma-Aldrich, 97%), iso-propanol [$(CH_3)_2CHOH$, Sigma-Aldrich, 99.7%], and nitric acid (HNO_3) were used without further purification. In this method, 20 mL of titanium tetra isopropoxide solution was added dropwise into 22 mL of a solution containing 10 mL of isopropanol and 12 mL of deionized water under constant stirring at 80 °C in a round-bottom flask. After 1 hour, 0.8 mL of concentrated nitric acid diluted with deionized water was added to the TTIP solution. The mixture was continuously stirred at 60 °C for 6 hours until a highly viscous sol–gel was formed. The prepared sol–gel was then heated at 300 °C for 2 hours in an open atmosphere. After annealing, approximately 2 g of TiO_2 nanocrystalline powder was obtained.

$$Ti(OCH(CH_3)_2)_4 + 2H_2O \rightarrow TiO_2 + 4(CH_3)_2CHOH$$

4. Applications of Metal Oxide Nanoparticles

4.1. Antimicrobial, Anticancer, and Cosmetic Properties of ZnO Nanoparticles

Zinc oxide nanoparticles (ZnO NPs) are among the most important metal oxide nanoparticles due to their wide range of biomedical applications. They exhibit significant antibacterial, antimicrobial, anti-inflammatory, anticancer, drug/gene delivery, cell imaging, and biosensing properties. [13-16] ZnO nanoparticles were initially utilized in the rubber industry because they improve the wear resistance, toughness, mechanical strength, and anti-ageing properties of rubber composites [16-17]. Due to their strong ultraviolet (UV) absorption capability, ZnO nanoparticles are extensively used in cosmetics and sunscreen formulations. Their excellent UV-blocking properties have also increased their application in the textile industry, where ZnO-coated fabrics exhibit antibacterial, deodorizing, and UV-resistant properties [18-19]. Zinc is an essential trace element present in various body tissues such as the brain, muscles, bones, and skin. It plays a vital role in enzymatic reactions, protein and nucleic acid synthesis, hematopoiesis, and neurogenesis. Nano-sized ZnO particles enhance zinc absorption in the body because of their small particle size. Consequently, nano-ZnO is widely used as a food additive [14-17]. Moreover, ZnO is classified as a "GRAS" (Generally Recognized as Safe) substance by the U.S. Food and Drug Administration (FDA). Owing to these beneficial properties, ZnO nanoparticles have attracted considerable attention in biomedical applications, including diabetes treatment and targeted drug delivery systems [18-20].

4.2. Antitumor Properties of Fe_3O_4 Nanoparticles

Superparamagnetic iron oxide nanoparticles (SPIO-NPs, Fe_3O_4) have emerged as promising materials for enhancing antitumor efficacy while reducing systemic side effects. Nanoparticulate drug delivery systems have gained significant attention in cancer nanotechnology because they enable the selective delivery of anticancer drugs to tumour tissues [21]. Various nanoparticulate carriers such as liposomes, polymeric micelles, and nanoparticles have been investigated for efficient cancer therapy. Swellable hydrophilic polymer nanoparticles are particularly attractive due to their nanoscale size (50–200 nm), high stability, and suitability for intracellular and intravenous drug delivery [22]. These systems can also encapsulate bioactive macromolecules such as proteins. One major challenge in cancer therapy is the reduced sensitivity of tumour cells to cytotoxic drugs. Therefore, polymeric nanospheres and magnetic nanoparticles have been developed to improve drug delivery efficiency and achieve site-specific targeting [23]. Superparamagnetic iron oxide nanoparticles possess excellent biocompatibility, chemical stability, low toxicity, and magnetic responsiveness, making them suitable for targeted and sustained drug delivery applications [24]. Amaneh J. et al. reported the successful entrapment of doxorubicin within SPIO nanoparticles modified with heparin for active targeting of cancer cells [25]. This modified nanoparticle system demonstrated promising potential in cancer treatment.

4.3. Catalytic and Regioselective Properties of Ag, Cu, Mn, Fe, and Co Nanocatalysts

Controlled regioselectivity is an important aspect in the synthesis of pharmaceutically significant molecules with defined regio- and stereoselectivity. Several methods have been developed for the synthesis of 3-ylidenephthalides and isocoumarins through conventional methods as well as C–H bond functionalization techniques [26]. In the regioselective synthesis involving 5-exo-dig and 6-endo-dig cyclization reactions, only a limited number of regioselective catalytic methods have been reported, including Cu^{2+}-nanocatalyzed and acid/base-controlled reactions [27-29]. Recently, Ag-based nanocatalysts have been employed in oxidative coupling and annulation reactions of benzoic acids with terminal alkynes, yielding 3-ylidenephthalides and isocoumarins with excellent yields and complete Z-selectivity through C–H bond activation mechanisms [30-34]. Transition metal nanoparticle catalysts such as Cu, Mn, Co, and Fe nanoparticles have attracted significant interest because of their high catalytic activity and unique reactivity compared to conventional Pd and Ni catalysts. Silver nanoparticles can coordinate simultaneously with triple bonds and electron-rich substituents such as Cl, Br, and OMe groups, thereby promoting regioselective cyclization reactions.

4.4. Microbicidal Properties of Ag Nanoparticles

Silver nanoparticles (Ag NPs) possess strong microbicidal activity against a broad spectrum of microorganisms. De Matteis et al. reported that the bactericidal effect of Ag NPs is dose-dependent [35]. Silver ions interact specifically with thiol groups present in cysteine residues of bacterial enzymes, thereby inhibiting essential metabolic pathways and leading to bacterial cell death. The antibacterial activity of Ag nanoparticles is strongly influenced by particle size. Smaller nanoparticles exhibit greater bactericidal activity because they can penetrate bacterial cell wall "pits" more effectively than larger particles [36].

Gurunathan et al. demonstrated that Ag nanoparticles with an average size of 5 nm showed stronger antibacterial activity than antibiotics such as ampicillin and vancomycin against certain bacterial strains [37-38]. Ag nanoparticles exhibit potent antibacterial activity against pathogens such as *Escherichia coli* O157:H7, *Streptococcus pyogenes*, *Salmonella enterica*, *Staphylococcus aureus*, and *Enterococcus faecalis* [39-40]. However, their activity against Gram-positive bacteria is comparatively weaker because the thick peptidoglycan layer in Gram-positive cell walls can trap silver ions and prevent their penetration into the cell membrane [41-42]. Environmental factors such as temperature, chlorine concentration, thiol groups, and oxygen-carrying proteins also influence the microbicidal activity of Ag nanoparticles.

4.5. Antiviral Properties of Ag Nanoparticles

Research on the antiviral properties of silver nanoparticles is comparatively limited, and the exact mechanism of antiviral action is still under investigation. Ag nanoparticles are believed to act primarily on the viral surface, preventing viral attachment and entry into host cells [40-43]. Particle size plays a critical role in antiviral efficacy. Speshock et al. reported that Ag nanoparticles ≤25 nm effectively inhibited arenavirus replication [44]. Similarly, Gaikwad et al. demonstrated that Ag nanoparticles ranging from 7–20 nm exhibited antiviral activity against herpes simplex virus (HSV-1 and HSV-2) and human parainfluenza virus type-3 [45]. Smaller nanoparticles showed superior antiviral activity compared to larger particles. Ag nanoparticles have also demonstrated inhibitory effects against HIV, influenza virus, and Monkeypox virus (MPV) [46-49]. Mori et al. reported that Ag nanoparticles ≤10 nm were effective against H1N1 influenza virus [32-33]. Interestingly, larger Ag nanoparticles (25–80 nm) were found to enhance MPV plaque formation, possibly due to nanoparticle agglomeration facilitating viral internalization [49-50] Therefore, nanoparticle size is a critical determinant in antiviral applications.

4.6. Applications for Healthcare Workers (HCWs)

Emerging infectious diseases (EIDs) such as Ebola virus disease (EVD), Middle East Respiratory Syndrome coronavirus (MERS-CoV), Severe Acute Respiratory Syndrome (SARS), MRSA infections, and cholera pose serious occupational hazards to healthcare workers (HCWs). During the Ebola outbreak in West Africa, a substantial number of healthcare workers were infected and many lost their lives [52]. MERS-CoV infections have also shown high fatality rates among HCWs [53]. Due to their broad-spectrum antimicrobial and antiviral activities, Ag nanoparticles have significant potential in protective healthcare applications. Ag nanoparticles generate reactive oxygen species (ROS) and release silver ions, leading to oxidative stress and microbial cell death. [50-51] Therefore, Ag NP-based materials can help reduce the risk of contact infections among healthcare workers. Researchers have developed microbicidal and antiviral materials by incorporating Ag nanoparticles onto chitin nanofiber sheets (CNFS) [34-55]. These materials exhibited strong antimicrobial activity against *E. coli* and antiviral activity against H1N1 influenza virus [32-55]. Such nanomaterials have potential applications in medical uniforms, protective gowns, masks, gloves, plastics, and surface disinfectant materials [48]. Although Ag NP-based protective materials show excellent antimicrobial performance, further studies are required to evaluate their long-term stability, safety, and potential effects on human health.

Conclusion

The sol–gel technique is an effective and versatile method for controlling material dimensions at the nanometer scale from the initial stages of synthesis. This method offers several advantages, including low-temperature processing, high purity, improved homogeneity, controlled morphology, net-shape casting, film coating, and fiber formation. Compared to conventional nanoparticle synthesis techniques, the sol–gel method is economical, flexible, and capable of producing nanoparticles with superior physicochemical properties. Metal oxide nanoparticles synthesized by the sol–gel technique exhibit promising biomedical and industrial applications, including anticancer, antibacterial, antiviral, anti-inflammatory, antidiabetic, drug delivery, bioimaging, catalytic, cosmetic, and textile applications. Therefore, sol–gel-derived metal oxide nanoparticles continue to be an important area of research in nanotechnology and pharmaceutical sciences.

References

1. Brinker C.J., and Scherer G.W., "The Physics and Chemistry of Sol-Gel Processing", Sol-Gel Science, 1990.
2. Davis P.J., Brinker C.J., Smith D.M., and Assink R.A., "Pore structure evolution in silica gel during aging / drying. II. Effect of pore fluids", J. Non-Cryst. Solids, vol 142, pp. 197-207, 1992.
3. Mohammad S., Md Hasibur R., Mohammad S.H., M. Afroza K., Aminul I., and M.H. Ara Begum, "Synthesis and Characterization of Silver Nanoparticles by Sol-Gel Technique," Nanoscience and Nanometrology, 2017.
4. H.N. Azlina, J.N. Hasnidawani, H. Norita and S.N. Surip, "Synthesis of SiO2 Nanostructures Using Sol-Gel Method," ACTA PHYSICA POLONICA A No. 4, Vol. 129, 2016.
5. J.N. Hasnidawani, H.N. Azlina, H. Norita, N.N. Bonnia, S. Ratim and E.S. Ali, "Synthesis of ZnO Nanostructures Using Sol-Gel Method", Procedia Chemistry, vol 19, pp. 211–216, 2016.
6. Zakiyyu I.T., Mohd K.M., Saliza A. and Khairunnadim A.S., "Preparation and Characterization of Magnetite (Fe3O4) nanoparticles By Sol-Gel Method," International Journal of Nanoelectronics and Materials, Vol. 12, No. 1, pp. 37-46, 2019.
7. Shakeel A., S.K. Hasanain, Nasia A., and M. Nadeem, "Synthesis of Fe2O3 nanoparticles by new Sol-Gel method and their structural and magnetic characterizations", 2016.
8. Fereydoun A., Seyed A.B., and Ali G., "Synthesis of alumina nano powder using sol-gel method and chelate precursor", Asian Academic Research Journal of Multidisciplinary, vol. 2, pp. 274-285, 2015.
9. Saja Mohsen Jabbar, "Synthesis of CuO Nano structure via Sol-Gel and Precipitation Chemical Methods", Al-Khwarizmi Engineering Journal, 2016.
10. Seyed J.D., Ramin K., Vahabodin G., and Farideh P., "Synthesis of Copper (II) Oxide (CuO) Nanoparticles and Its Application as Gas Sensor", Journal of Applied Biotechnology Reports, Vol 2(4), pp. 329-332, 2015.
11. Zainab N.J., and Adawiya J.H., Samar Y., "Synthesis of TiO2 Nan particles by Using Sol-Gel Method and its Applications as Antibacterial Agents", 4th International Scientific Conference on Nanotechnology & Advanced Materials Their Applications (ICNAMA), pp. 3-4, 2013.
12. Ajay S., R.K. Karn, and S.K. Paniyadn, "Synthesis of TiO2 Nanoparticles by Sol-gel Method and Their Characterization", Journal of Basic and Applied Engineering Research, Vol 1, pp. 1-5, 2014.
13. P.K. Mishra, H. Mishra, A. Ekielski, S. Talegaonkar, and B. Vaidya, "Zinc oxide nanoparticles: a promising nanomaterial for biomedical applications," Drug Discovery Today, 1825–1834, 2017.
14. T.G. Smijs and S. Pavel, "Titanium dioxide and zinc oxide nanoparticles in sunscreens: focus on their safety and effectiveness," Nanotechnology, Science and Applications, vol. 4, pp. 95–112, 2011.
15. J.A. Ruszkiewicz, A. Pinkas, B. Ferrer, T.V. Peres, A. Tsatsakis, and M. Aschner, "Neurotoxic effect of active ingredients in sunscreen products, a contemporary review," Toxicology Reports, vol. 4, pp. 245–259, 2017.
16. A. Kolodziejczak-Radzimska and T. Jesionowski, "Zinc oxide–from synthesis to application: a review," Materials, vol. 7, no. 4, pp. 2833–2881, 2014.
17. S. Sahoo, M. Maiti, A. Ganguly, J.J. George, and A.K. Bhowmick, "Effect of zinc oxide nanoparticles as cure activator on the properties of natural rubber and nitrile rubber," Journal of Applied Polymer Science, vol. 105, no. 4, pp. 2407–2415, 2007.
18. M.D. Newman, M. Stotland, and J.I. Ellis, "The safety of nanosized particles in titanium dioxide- and zinc oxide based sunscreens," Journal of the American Academy of Dermatology, vol. 61, no. 4, pp. 685–692, 2009.
19. A. Hatamie, A. Khan, M. Golabi et al., "Zinc oxide nanostructure-modified textile and its application to biosensing, photocatalysis, and as antibacterial material," Langmuir, vol. 31, no. 39, pp. 10913–10921, 2015.
20. J.W. Rasmussen, E. Martinez, P. Louka, and D.G. Wingett, "Zinc oxide nanoparticles for selective destruction of tumor cells and potential for drug delivery applications," Expert Opinion on Drug Delivery, vol. 7, no. 9, pp. 1063–1077, 2010.
21. M. Ferrari, "Cancer nanotechnology: opportunities and challenges," Nat Rev Cancer, vol. 5, pp. 161–71, 2005.
22. S. Kommareddy, and M. Amiji, "Preparation and evaluation of thiolmodified gelatin nanoparticles for intracellular DNA delivery in response to glutathione," Bioconjug. Chem., vol. 16, 1423–1432, 2005.
23. R.J. Linhardt, "Heparin-induced cancer cell death," Chem. Biol., vol. 11, pp. 420–422, 2007.
24. M.K. Yu, D.Y. Lee, Y.S. Kim, K. Park, S.A. Park, and D.H. Son, "Antiangiogenic and apoptotic properties of a novel amphiphilic folate–heparin–lithocholate derivative having cellular internality for cancer therapy," Pharm. Res., vol. 24, pp. 705–14, 2007.
25. Amaneh J., Shahin A., Ali A. Saboury, and Saeed R., "Anticancer Effect of Doxorubicin Loaded Heparin based Super-paramagnetic Iron oxide Nanoparticles against the Human Ovarian Cancer Cells", World Academy of Science, Engineering and Technology, vol. 74, pp. 145-149, 2014.
26. (a) D. Rambabu, G.P. Kumar, B.D. Kumar, R. Kapavarapu, M.V.B. Rao and M. Pal, Tetrahedron Lett., vol. 54, 2989–2995, 2013. (b) S. Dhara, R. Singha, M. Ghosh, A. Ahmed, Y. Nuree, A. Das and J.K. Ray, RSC Adv., vol. 4, 42604–42607, 2014.
27. (a) V. Subramanian, V.R. Batchu, D. Barange and M. Pal, J. Org. Chem., vol. 70, pp. 4778–4783, 2005. (b) L. Zhou and H.-F. Jiang, Tetrahedron Lett., vol. 48, pp. 8449–8452, 2007.
28. M. Jithunsa, M. Ueda and O. Miyata, Org. Lett., vol. 13(3), pp. 518–521, 2011.
29. M. Uchiyama, H. Ozawa, K. Takuma, Y. Mastumoto, M. Yonehara, K. Hiroya and T. Sakamoto, Org. Lett., vol. 8(24), pp. 5517–5520, 2006.
30. Sandeep C., Bharti Rajesh K.S., Lalit Y., Mohit K.T., and Krishan K., The Royal Society of Chemistry, vol. 8, pp. 23152–23162, 2018.
31. Y. Liu, Y. Yang, Y. Shi, X. Wang, L. Zhang, Y. Cheng and J. You, Organometallics, vol. 35(10), pp. 1350–1353, 2016.
32. Mori Y., Ono T., Miyahira Y., Nguyen V.Q., Matsui T. and Ishihara M., "Antiviral activity of silver nanoparticle/chitosan composites against H1N1 influenza A virus", Nanoscale Res. Lett., 2013. [PubMed]

33. Mori Y., Tagawa T., Fujita M., Kuno T., Suzuki S., Matsui T. and Ishihara M., "Simple and environmentally friendly preparation and size control of silver nanoparticles using an inhomogeneous system with silver-containing glass powder", J. Nanopart. Res., vol. 13, pp. 2799–2806, 2011.
34. Ishihara M., Nguyen V.Q., Mori Y., Nakamura S. and Hattori H., "Adsorption of Silver Nanoparticles onto Different Surface Structures of Chitin/Chitosan and Correlations with Antimicrobial Activities", Int. J. Mol. Sci., vol. 16, pp. 13973–13988, 2015.
35. De Matteis V., Malvindi M.A., Galeone A., Brunetti V., De Luca E., Kote S., Kshirsagar P., Sabella S., Bardi G. and Pompa P.P., "Negligible particle-specific toxicity mechanism of silver nanoparticles: The role of Ag+ ion release in the cytosol", Nanomedicine, vol. 11, pp. 731-739, 2015.
36. Nguyen V.Q., Ishihara M., Nakamura S., Hattori H., Ono T., Miyahira Y. and Matsui T., "Interaction of silver nanoparticles and chitin powder with different sizes and surface structures: The correlation with antimicrobial activities", J. Nanomater, vol. 13, 2013.
37. Ramar M., Manikandan B., Marimuthu P.N., Raman T., Mahalingam A., Subramanian P., Karthick S. and Munusamy A., "Synthesis of silver nanoparticles using Solanum trilobatum fruits extract and its antibacterial, cytotoxic activity against human breast cancer cell line MCF 7", Spectrochim. Acta A., vol. 140, pp. 223–228, 2015.
38. Gurunathan S., Han J.W., Kwon D.N. and Kim J.H., "Enhanced antibacterial and anti-biofilm activities of silver nanoparticles against Gram-negative and Gram-positive bacteria", Nanoscale Res. Lett., vol. 9, p. 373, 2014.
39. Shameli K., Ahmad M.B., Zargar M., Yunus W.M., Rustaiyan A. and Ibrahim N.A., "Synthesis of silver nanoparticles in montmorillonite and their antibacterial behavior", Int. J. Nanomed., vol. 6, pp. 581-590, 2011.
40. Karmali M.A., "Factors in the emergence of serious human infections associated with highly pathogenic strains of shiga toxin-producing Escherichia coli", Int. J. Med. Microbiol., vol. 308, pp. 1067-1072, 2018.
41. Devi L.S., and Joshi S.R., "Antimicrobial and synergistic effects of silver nanoparticles synthesized using soil fungi of high altitudes of eastern Himalaya", Mycobiology, vol. 40, pp. 27-34, 2012.
42. Velusamy P., Su C.H., Venkat Kumar G., Adhikary S., Pandian K., Gopinath S.C., Chen Y. and Anbu P., "Biopolymers Regulate Silver Nanoparticle under Microwave Irradiation for Effective Antibacterial and Antibiofilm Activities". PLOS ONE., vol. 11, 2016.
43. Mehrbod P., Motamed N., Tabatabaian M., Estyar R.S., Amini E., Shahidi M. and Kheiri M., "In vitro antiviral effect of "nanosilver" on influenza virus", DARU J. Pharm. Sci., vol. 17, pp. 88-93, 2009.
44. Speshock J.L., Murdock R.C., Braydich-Stolle L.K., Schrand A.M. and Hussain S.M., "Interaction of silver nanoparticles with Tacaribe virus", J. Nanobiotechnol., vol. 8, p. 19, 2010.
45. Gaikwad S., Ingle A., Gade A., Rai M., Falanga A., Incoronato N., Russo L., Galdiero S. and Galdiero M., "Antiviral activity of mycosynthesized silver nanoparticles against herpes simplex virus and human parainfluenza virus type 3", Int. J. Nanomed., vol. 8, pp. 4303-4314, 2013.
46. Baram-Pinto D., Shukla S., Perkas N., Gedanken A. and Sarid R., "Inhibition of herpes simplex virus type 1 infection by silver nanoparticles capped with mercaptoethane sulfonate", Bioconjug. Chem., vol. 19, pp. 1497-1502, 2009.
47. Lara H.H., Ayala-Nunez N.V., Ixtepan-Turrent L. and Rodriguez-Padilla C., "Mode of antiviral action of silver nanoparticles against HIV-1", J. Nanobiotechnol., vol. 8(1), 2010.
48. Elechiguerra J.L., Burt J.L., Morones J.R., Camacho-Bragado A., Gao X., Lara H.H. and Yacaman M.J., "Interaction of silver nanoparticles with HIV-1" J. Nanobiotechnol., vol. 3(6), 2005.
49. Rogers J.V., Parkinson C.V., Choi Y.W., Speshock J.L. and Hussain S.M., "A preliminary assessment of silver nanoparticle inhibition of monkeypox virus plaque formation", Nanoscale Res. Lett., vol. 3, pp. 129-133, 2008.
50. Kora A.J. and Sashidhar R., "Biogenic silver nanoparticles synthesized with rhamnogalacturonan gum: Antibacterial activity, cytotoxicity and its mode of action", Arab. J. Chem., vol. 11, pp. 313-323, 2018.
51. Kinoda J., Ishihara M., Hattori H., Nakamura S., Fukuda K. and Yokoe H., "Cytotoxicity of Silver Nanoparticle and Chitin-Nanofiber Sheet Composites Caused by Oxidative Stress", Nanomaterials, vol. 6, p. 189, 2016.
52. Green A., "Remembering health workers who died from Ebola in 2014", Lancet., vol. 384, pp. 2201-2206, 2014.
53. Al-Tawfiq J.A. and Memish Z.A., "Middle East respiratory syndrome coronavirus in the last two years: Health care workers still at risk", Am. J. Infect. Control., 2019.
54. Clement R., "Is it time for an evidence-based uniform for doctors?", BMJ., vol. 345, e8286, 2012.
55. Nguyen V.Q., Ishihara M., Kinoda J., Hattori H., Nakamura S., Ono T., Miyahira Y. and Matsui T., "Development of antimicrobial biomaterials produced from chitin-nanofiber sheet/silver nanoparticle composites", J. Nanobiotechnol., vol. 12(49), 2014.